Supporting Information

Spatial Separation Co-catalysts for Efficient Charge Separation: Hollow Pt/CdS/N-ZnO/CoO_x Graphene Microtubule with High Stability for Photocatalytic Reaction

Yong Liang[a,b], Yuexing Chen[a], Maojun Zhao[a], Li Lin[a], Rongtao Duan[a], Yuanyuan Jiang[a], Jun Yan[b], Ying Wang[c], Jun Zeng[d], Yunsong Zhang[a,*]

[a]College of Science, Sichuan Agricultural University, Yaan 625014, China

[b]College of Pharmacy and Biological Engineering, Chengdu University, Chengdu 610106, China

[c]College of Water Conservancy and Hydropower Engineering, Sichuan Agricultural University, Yaan 625014, China

[d]Key Laboratory of Green Chemistry of Sichuan Institutes of Higher Education, Sichuan University of Science and Engineering, Zigong 643002, China

[*]Corresponding author: Tel: +86 835 2885782; Fax: +86 835 2862227; Email address: yaanyunsong@126.com

1 Method

1.1. Characterizations

X-ray diffraction analysis was performed on a DX-2600 X-ray diffractometer. The morphology and surface elements distribution of Pt/CdS/ZnO/CoO_x graphene microtubule was observed by a scanning electron microscopy (SEM, JSM-7500F, Japan). Additionally, the Fourier transform infrared spectra were used to evaluate the surface functional groups of the samples (FTIR, Shimaduzu-8400S, Japan) and the X-ray photoelectron spectroscopy (XPS, XSAM800, Britain) was applied to measure the

surface chemical composition, respectively. Raman spectra were acquired on a Raman system (Thermo Scientific, DXR Smart, USA). The UV-visible diffuse reflectance spectra (DRS, using $BaSO_4$ as the standard reference) were carried out on a Lambda75 UV-Vis spectrophotometer. Photoluminescence (PL) spectra were detected with FLS1000 Edinburgh Instrument. The electrochemical impedance spectroscopy (EIS) measurements were measured with an electrochemical workstation (CHI-660c, China).

2 Supplementary Results and Discussion

2.1 FTIR spectra and Roman spectra of samples

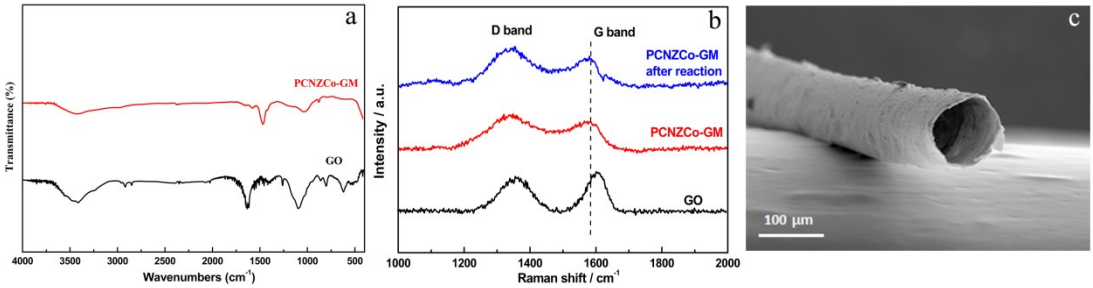

Fig. S1 (a) FTIR spectra of PCNZCo-GM and GO, (b) Roman spectra of PCNZCo-GM, PCNZCo-GM after reaction and GO, (c) SEM image of PCNZCo-GM after reaction

2.2 XPS analysis of samples

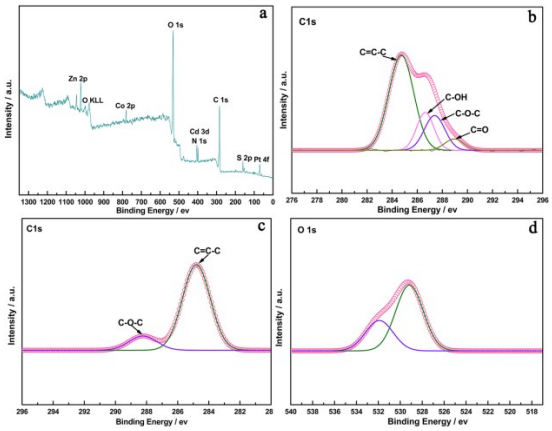

Fig. S2 (a) Full-scale XPS survey spectrum of PCNZCo-GM, (b, c) XPS spectra of C1s of GO and PCNZCo-GM and (d) XPS spectra of O1s of PCNZCo-GM.

2.3 Band-gap estimation

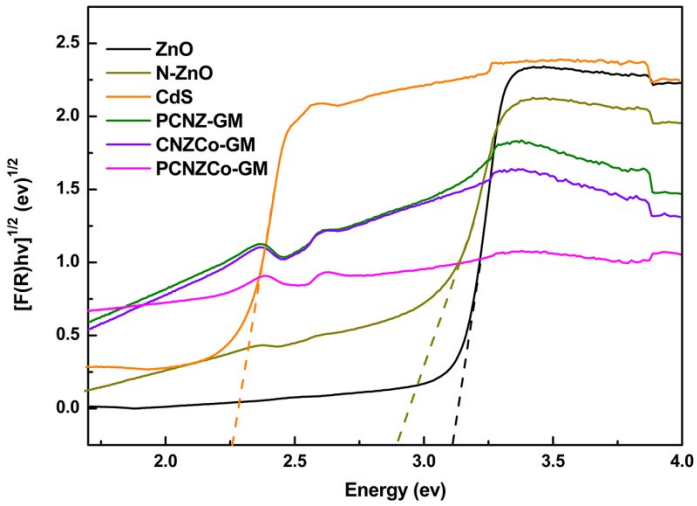

Fig. S3 Plots of $[F(R)hv]^2$ vs. the energy of samples.

As shown in Figure S4, the band gap energy of CdS and N-ZnO crystals were estimated to about 2.26 eV and 2.89 eV, respectively. Meanwhile, the band edge positions of conduction band (CB) and valence band (VB) of it can be calculated by the following Eqs. (2), (3):

$$E_{CB} = X - E_C - 0.5E_g \quad (1)$$

$$E_{VB} = E_g + E_{CB} \quad (2)$$

where, E_{CB} is the CB edge potential, E_{VB} is the VB edge potential, X is the electronegativity of the semiconductor, which is the electronegativity geometric mean of the constituent atoms (5.19 eV for CdS and 5.79 eV for ZnO), E_C is the energy of free electrons on the hydrogen scale (about 4.5 eV), and Eg is the band gap energy of the semiconductor). According to Eqs. (1) and (2), the CB and VB edge potentials of CdS are -0.44 eV and 1.82 eV, respectively, and N-ZnO are supposed to be -0.16 eV and 2.73 eV.

2.4 Photocatalytic ability of samples with different N-ZnO

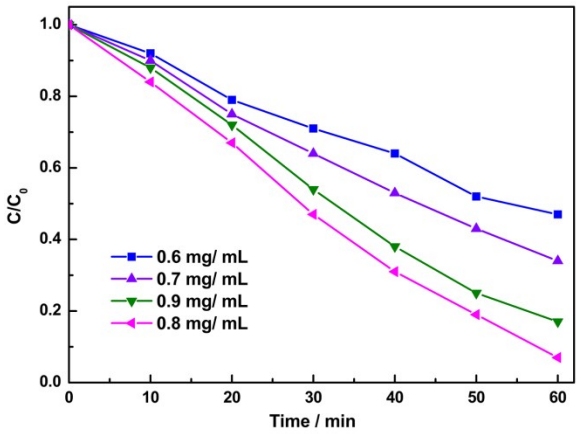

Fig. S4 The degradation dynamics curves of PCNZCo-GM with different content of N-ZnO. The respective amount of the N-ZnO precursors in the hybrid preparation is as follows: 0.6 mg/mL, 0.7 mg/mL, 0.8 mg/mL, and 0.9 mg/mL.

2.5 Total organic carbon (TOC) removal efficiency

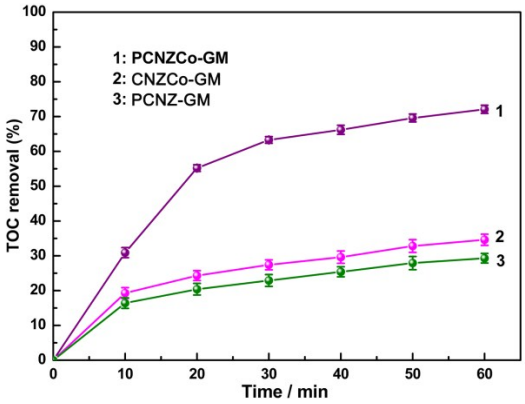

Fig. S5 Total organic carbon (TOC) removal efficiency during the photodegradation process.

2.6 Degradation dynamics curves and recycling tests of colorless BPA

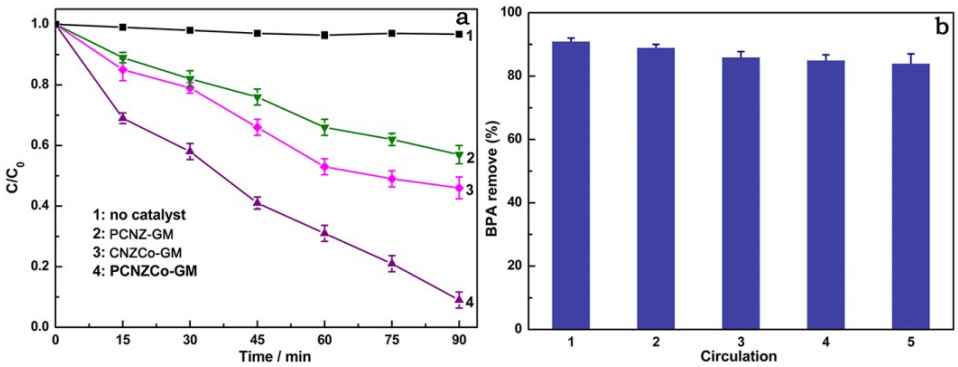

Fig. S6 (a) Photocatalytic degradation curves of BPA and (b) recycling properties of photodegrading BPA over the PCNZCo-GM.

2.7 The trapping experiments

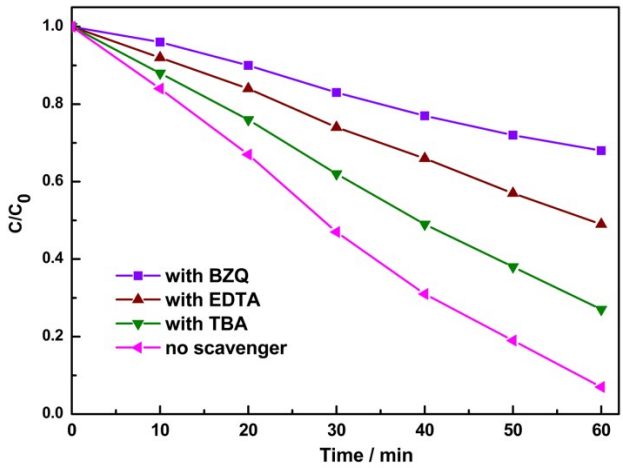

Fig. S7 The trapping experiments of the PCNZCo-GM.

2.8 Photocatalytic performance comparisons of CdS or ZnO-based composites

Some researchers have reported the construction of CdS or ZnO-based heterojunctions, such as CF@ZnO/CdS,[1] CdS/g-C_3N_4,[2] RGO/ZnO,[3] etc., which enhance the photocatalytic performance than single photocatalysts. Effective separation of charge and high cycle stability are key factors for photocatalysts application. In this paper, we prepared a spatially separated hollow Pt/CdS/ZnO/CoO_x graphene microtube (PCNZCo-GM) with a double cocatalysts by capillary and hydrothermal method for enhancing charge separation efficiency and photocatalytic oxidation ability. Our method has significant advantage compared with traditional methods because it enables easy inhalation of solution by capillary action and efficient separation of cocatalysts. In the spatial separation composite, Pt as electron collectors and CoO_x as hole collectors were selectively decorated on the inner and outer surfaces of CdS/N-ZnO double-layered graphene microtubule (CNZ-GM), which prompts photogenerated electrons and holes near the surface to move in the opposite direction. The absorption range of ZnO can be significantly expanded by nitrogen doping and the charge separation can be effectively promoted by the

construction of Z-scheme heterojunction between CdS and N-ZnO. The hollow graphene microtubule structure with an oxidation-reduction co-catalyst supported on its inner and outer surfaces is conducive to simultaneous exposure of redox surface, charge separation, reusability and mass transfer in photocatalytic process. Combining other merits, such as excellent structural and functional characteristics of CdS and N-ZnO, large surface area and surface reaction kinetics promoted by cocatalysts, the PCNZCo-GM is an excellent photocatalyst of both photodegradation and disinfection. Compared with other CdS or ZnO-based photocatalysts, the PCNZCo-GM exhibits a more excellent photodegradation performance, rapider antibacterial performance and higher recycling stability (Table S1). Consequently, the PCNZCo-GM shows a great merit as a novel effective catalyst for water purification.

Table S1. Photocatalytic performance comparisons of the PCNZCo-GM with representative CdS or ZnO based composites.

Catalyst category	$C_{catalyst}$	Dyes/bacterial species	Reaction conditions	Degradation performance	Disinfection activity	Recycling Stability
CF@ZnO/CdS [1]	5.17 g L^{-1}	RhB (100 mL, 10 mg/L)	500 W, Xe lamp, $\lambda < 420$ nm	90%, 60min	-	3rd run, 80%
RGO/ZnO [3]	0.1 g L^{-1}	RhB (100 mL, $1.00*10^{-5}$ M)	Xe lamp	97.5%, 120 min	-	4th run, 95.5%
Ag/ZnO/g-C_3N_4 [4]	100μg/ mL	*E. coli*	300 W, Xe lamp, $\lambda > 400$ nm	-	10^7, 120 min	3rd run, 6.12 log inactivated
BiOCl-Au-CdS [5]	1 g L^{-1}	MO (50 mg/L,20 mg/L)	300 W, Xe lamp, (AM1.5)	98%, 180 min	-	-
Fe_2O_3/ZnO/$ZnFe_2O_4$ [6]	0.6 g L^{-1}	RhB/MO (50 mL, 20 mg/L)	500 W, halide lamp, $\lambda > 420$ nm	95.7%/52.3%, 1h	-	3rd run, 88.9%
This work	0.7 g L^{-1}	MO (70 mL, 10 mg/L) *E. coli*	500 W, Xe lamp, $\lambda > 420$ nm	95%, 60 min	10^7, 60 min	5th run, 96%, 6.63 log inactivated

Reference

1. Z. J. Yu, M. R. Kumar, Y. Chu, H. X. Hao, Q. Y. Wu and H. D. Xie, *ACS Sustainable Chem. Eng.*, 2018, **6**, 155-164.
2. X. Yao and W. D. Zhang, *Eur. J. Inorg. Chem.*, 2015, **2015**, 1744-1751.
3. Z. Dawei, Z. Yi, D. Yuehong, X. Ye, Z. Ya, Z. Zhen and Z. Dandan, *ChemistrySelect*, 2018, **3**, 8740-8747.
4. S. Ma, S. Zhan, Y. Xia, P. Wang, Q. Hou and Q. Zhou, *Catal. Today*, 2019, **330**, 179-188.
5. Q. Li, Z. Guan, D. Wu, X. Zhao, S. Bao, B. Tian and J. Zhang, *ACS Sustainable Chem. Eng.*, 2017, **5**, 6958-6968.
6. X. Li, B. Jin, J. Huang, Q. Zhang, R. Peng and S. Chu, *Solid State Sci.*, 2018, **80**, 6-14.